6390–6402 *Nucleic Acids Research, 2011, Vol. 39, No. 15* *Published online 4 May 2011*
doi:10.1093/nar/gkr266

Dimer formation and conformational flexibility ensure cytoplasmic stability and nuclear accumulation of Elk-1

Emma L. Evans[1], Janice Saxton[1], Samuel J. Shelton[1], Andreas Begitt[1], Nicholas D. Holliday[1], Robert A. Hipskind[2] and Peter E. Shaw[1,*]

[1]School of Biomedical Sciences, Queen's Medical Centre, Nottingham, NG7 2UH, UK and [2]Institut de Génétique Moléculaire de Montpellier, CNRS, UMR5535, 1919 route de Mende, 34293 - Montpellier Cedex 05, France

Received November 26, 2010; Revised April 5, 2011; Accepted April 6, 2011

ABSTRACT

The ETS (E26) protein Elk-1 serves as a paradigm for mitogen-responsive transcription factors. It is multiply phosphorylated by mitogen-activated protein kinases (MAPKs), which it recruits into pre-initiation complexes on target gene promoters. However, events preparatory to Elk-1 phosphorylation are less well understood. Here, we identify two novel, functional elements in Elk-1 that determine its stability and nuclear accumulation. One element corresponds to a dimerization interface in the ETS domain and the second is a cryptic degron adjacent to the serum response factor (SRF)-interaction domain that marks dimerization-defective Elk-1 for rapid degradation by the ubiquitin–proteasome system. Dimerization appears to be crucial for Elk-1 stability only in the cytoplasm, as latent Elk-1 accumulates in the nucleus and interacts dynamically with DNA as a monomer. These findings define a novel role for the ETS domain of Elk-1 and demonstrate that nuclear accumulation of Elk-1 involves conformational flexibility prior to its phosphorylation by MAPKs.

INTRODUCTION

A major pre-occupation of studies on transcription is how acutely regulated factors increase the rate of initiation at target gene promoters. The consensus view is that they facilitate the assembly of promoter complexes by the basal transcription machinery and the RNA polymerase II holoenzyme (RNAPII) in a manner dependent on their post-translational modification. In this regard phosphorylation-dependent activation of transcription by the ETS protein Elk-1, a nuclear target for mitogen-activated protein kinases (MAPKs) and transcriptional activator of immediate early genes such as c-*fos* (1,2), is a well-established model, although an understanding of the molecular mechanisms is far from complete. One of several non-exclusive models invokes conformational change in the protein, for which there is limited evidence (3–5). Another is based on Elk-1 de-sumoylation (6), a modification linked to the establishment of sub-nuclear architecture (7). A third scenario involves the recruitment of enzymatic activities to promoters by Elk-1 (e.g. histone acetyltransferases, protein kinases) to bring about activation (8,9) and a fourth describes the phosphorylation-dependent recruitment of the Mediator/RNAPII complex via interactions with MED23 (Sur2) (10). Additional studies have highlighted the dynamic nature of gene transcription and its attendant regulatory processes: high mobility and rapid turnover are cited as characteristics associated with some acutely regulated nuclear hormone receptors (11,12). It is therefore apparent that events preceding acute stimulation may be as important for the overall function of some transcription factors as subsequent events potentially linked to their recycling.

Although much information has been accrued on the recognition and phosphorylation of nuclear Elk-1 by MAPKs, insights into the stages preceding its activation are lacking. For this reason we sought to identify factors that affect the nuclear pool of latent Elk-1. Here we show that Elk-1 contains two motifs that determine its stability and consequent accumulation in the nucleus or its rapid degradation in the cytoplasm. Furthermore, Elk-1 undergoes a conformational transition upon nuclear entry, as in the nucleus Elk-1 appears to be a monomer undergoing dynamic DNA interactions that may contribute to nuclear accumulation. These findings highlight the importance of conformation and stability in establishing a nuclear pool of latent Elk-1 for activation by MAPKs.

*To whom correspondence should be addressed. Tel: +44 115 8230120; Fax: +44 115 8230142; Email: peter.shaw@nottingham.ac.uk

MATERIALS AND METHODS

Cell culture, transfections and extract preparation

HEK293, COS1, HeLa, U2OS, E36 and E36(*ts20*) cells were grown in Dulbecco's MEM supplemented with 10% foetal calf serum (FCS), 2 mM *L*-glutamine, 100 U ml^{-1} penicillin and 100 µg ml^{-1} streptomycin. Cells were transfected according to standard procedures. For routine analysis of protein expression, cells were washed in cold PBS and lysed directly in Laemmli loading buffer. For cell fractionation, nuclear and cytoplasmic extracts were prepared as described earlier (13). For ubiquitylation assays, cells were lysed in denaturing buffers containing 6 M guanidinium hydrochloride and ubiquitin conjugates were isolated by immobilized metal affinity chromatography (IMAC).

Plasmids

Expression of Elk-1 and its derivatives was from pCMV5 or pcDNA3 based vectors. The Elk-DM contains the mutations R65A, Y66F; Elk-SM contains the mutations L158P, Y159A. Ets-1 and PU.1 YFPn/c fusions were also expressed from pCMV5. Plasmids were constructed by standard recombinant DNA procedures and all sequences generated by PCR were verified by DNA sequencing. Further information on individual plasmids can be obtained upon request.

Antibodies

The anti-Elk-1 antibodies used were a rabbit polyclonal developed in house (ElkC), from Sigma and Santa Cruz (H160). The anti-TBP was from Santa Cruz (N-12); the anti-Tubulin was from Santa Cruz (TU-20); the anti-Actin was from Sigma (A2060); the anti-HA rat monoclonal was from Roche (3F10); the anti-GST monoclonal was from Cell Signalling (26H1); the anti-GFP was from Clontech.

Polysome fractionation and northern blotting

Sucrose gradient centrifugation was used to separate ribosomes into polysomal and sub-polysomal forms. Gradients were fractionated with continuous monitoring at 260 nm and RNA was isolated from each fraction as described (14). Northern blotting was performed as described previously (15).

Expression and purification of recombinant proteins

Cell-free translation of Elk-1 and sElk was performed with the TNT coupled system (Promega). Bacterial expression of recombinant Elk-1/purification by IMAC and expression of GST-fusion proteins/coupling to glutathione agarose have been described earlier (16). The HA-tagged Δ17-23 mutant of Elk-ets domain and sElk were purified by IMAC under denaturing conditions (8 M urea), which was slowly reversed by stepwise dialysis. When purified and refolded under the same conditions, the recombinant HA-Elk-ets was at least as active for DNA binding to the E74 duplex as when purified under native conditions.

Gel filtration

Gel filtration experiments with Elk-1 and sElk were performed on a superose 12 HR 10/30 column as described earlier (3). For experiments with the recombinant Elk-ets domain, 25 mM HEPES pH 7.5, 10 mM $MgCl_2$, 0.1% NP-40 with 50 mM KCl (low salt) or 250 mM KCl (high salt) was used. To facilitate cross-dimerization Elk-1 and Elk-ets domain were precipitated in ethanol at a 1:5 ratio, denatured in low salt buffer with 8 M urea and renatured by stepwise dialysis to remove urea.

SDS–PAGE and immunoblotting

Proteins were transferred from denaturing polyacrylamide gels by semi-dry electro-transfer (BioRad) to PVDF membranes and probed with antibodies using standard protocols.

DNA binding and protein interaction assays

Electrophoretic Mobility Shift Assays (EMSAs) were performed as described previously (16). GST pull-downs were performed as described (17) with slight modifications. The oligonucleotides used to generate the E74 binding site and control duplex lacking an ETS consensus were as follows:

E74U 5′-CTAGAGCTGAATAACCGGAAGTAACT CAT
E74L 5′-CTAGATGAGTTACTTCCGGTTATTCAGCT
CON-U 5′-AGACCAACATGAATTACGACAGGCT CAGCCGGG
CON-L 5′-CCCGGCTGAGCCTGTCGTAATTCATG TTGGTCT

Confocal microscopy, FRAP and FLIP

Images of bimolecular fluorescence complementation (BiFC) were obtained on a Zeiss LSM510 scanning confocal microscope or an Axiovert S100 and AxioCam digital camera from HeLa cells grown on glass-bottomed dishes (Iwaki) after transfection with polyethyleneimine (PEI) and incubation for 12–16 h at 30°C. For FRAP and FLIP experiments, HeLa cells were cultured and transfected as described but analyses were performed on a Leica CLSM.

RESULTS

Amino-terminal truncations destabilize Elk-1

This study originated with the observation that amino-terminal truncations of Elk-1, including the neuronal-specific isoform (sElk), failed to accumulate as anticipated when expressed ectopically in cells. As *elk-1* RNA undergoes alternative splicing (18) a possible cause of this phenomenon could be regulation of translation initiation. However, the absence of the 5′-UTR from the expression constructs used suggested that post-translational regulation might also be involved.

To scrutinize these options more closely, we first transfected pCMV5-based expression constructs for Elk-1 and

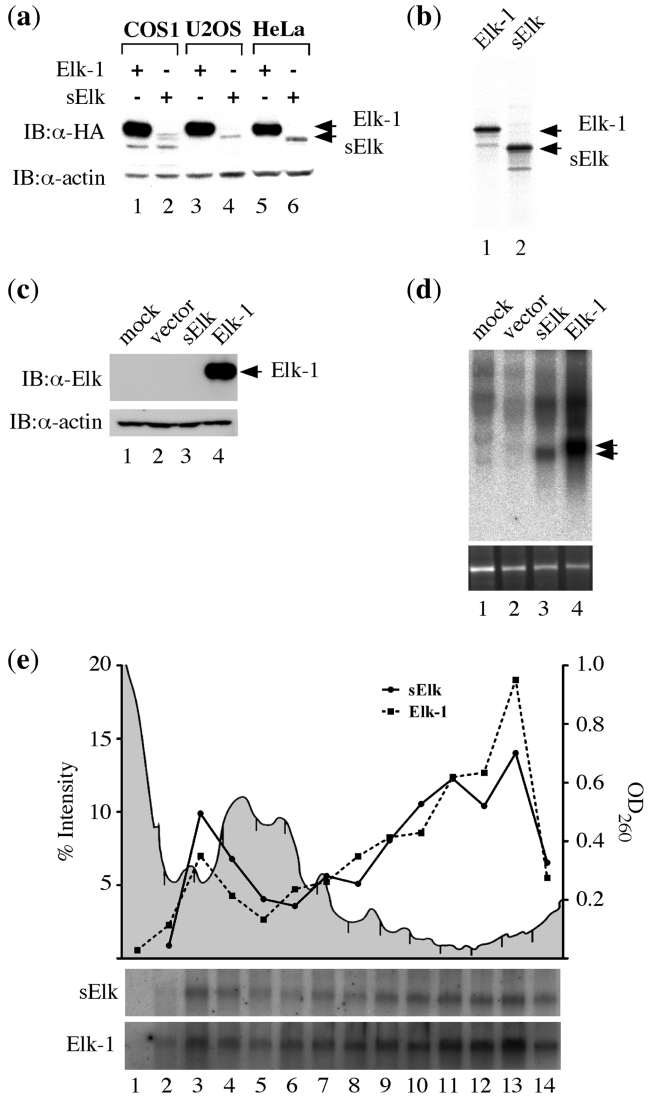

Figure 1. Differential accumulation of Elk-1 and sElk. (**a**) COS1, U2OS and HeLa cells were transfected with pCMV5-based expression vectors for Elk-1 (lanes 1, 3 and 5) or sElk (lanes 2, 4 and 6). After 48 h whole cell lysates were prepared and Elk-1 expression was monitored by SDS–PAGE and immunoblotting. Lower panels show actin re-probes as loading controls. (**b**) ^{35}S-labelled Elk-1 (lane 1) and sElk (lane 2) were expressed from pcDNA3-based vectors in a cell-free system and analysed by SDS–PAGE. (**c**) HEK293 cells were mock transfected, transfected with pcDNA3 (vector) or the expression vectors for sElk and Elk-1 used in (b) and expression was analysed by SDS–PAGE and immunoblotting. (**d**) RNA was prepared from HEK293 cells transfected as in (c) and analysed by northern blot. Lower panel shows 18S RNA. (**e**) Lysates of cells transfected as in (c) and (d) were separated by sucrose gradient centrifugation and fractions were analysed for total RNA content (OD_{260}) and Elk-1/sElk mRNA by northern blot.

sElk with amino-terminal haemaglutinin (HA) tags into several cell lines. In all cases, Elk-1 accumulated whereas sElk was present only at much lower levels (Figure 1a). In cell-free transcription and translation reactions programmed with analogous pcDNA3-based expression plasmids differing only in the presence or absence of coding sequences for Elk-1 residues 1–54, no difference in expression of the two proteins was observed (Figure 1b) although from these vectors the expression levels in HEK293 cells differed profoundly (Figure 1c).

To determine if the failure of sElk to accumulate in cells was due to the absence of stable mRNA or lack of translation, we compared the levels of Elk-1 and sElk RNA (Figure 1d) and their distribution across polysome fractions (Figure 1e). In several independent experiments more Elk-1 than sElk mRNA was detected (~9-fold), indicating that transcription and/or processing of sElk mRNA was somewhat less efficient than Elk-1 mRNA. Nonetheless, the polysomal distributions of Elk-1 and sElk mRNA were very similar, with only a slightly higher percentage of Elk-1 mRNA present in the largest polysomes, indicating that sElk mRNA is actively translated in HEK293 cells. These results indicate that the differential accumulation of these two proteins is unlikely to be due to disparate rates of translation.

Incorrectly folded proteins are recognized by post-translational quality control mechanisms (19,20) and an incomplete ETS domain could conceivably target N-terminal Elk-1 truncations for degradation. However, Elk-1 proteins lacking the entire ETS domain and the flexible linker between ETS domain and SRF interaction domain (SID, see Supplementary Figure S1a), which is unstructured in Sap1a/SRF co-crystals (21,22), also failed to accumulate in HEK293 cells (Supplementary Figure S1b, lanes 2, 4 and 6). Failure of amino-terminal Elk-1 truncations to accumulate could have been due to defective nuclear import, so each mutant was fused to an ectopic nuclear localisation signal (NLS). However, the presence of an NLS caused no significant change in the accumulation of truncated Elk-1 proteins (Supplementary Figure S1b, lanes 3, 5 and 7).

sElk is rapidly turned over by the 26S proteasome

The failure of N-terminal Elk-1 truncations to accumulate in cells could be due to their rapid turnover. Treatment of cells for 16 h with MG132, an inhibitor of the proteasome (23), significantly increased the level of sElk (Figure 2a compare lanes 2 and 4), whereas neither Elk-1 nor sElk appeared to be stabilized by Bafilomycin, an inhibitor of autophagy (lanes 5 and 6). When his-tagged versions of Elk-1 and sElk were co-expressed with HA-tagged ubiquitin and isolated from denatured cell lysates by IMAC, poly-ubiquitylated species of both proteins were detected (Figure 2b, lanes 2 and 5) and treatment of cells with MG132 selectively increased the amount of poly-ubiquitylated sElk (lane 6).

To confirm a role for the ubiquitin–proteasome system (UPS) in rapid sElk turnover, we used a hamster cell line expressing a temperature-sensitive version of the E1 ubiquitin-activating enzyme (E36 *ts*20) (24). In the parental cell line (E36) little difference was seen in Elk-1 and sElk levels between the permissive and non-permissive temperatures (Figure 2c, compare lanes 1 and 2 with 3 and 4), but in the *ts*20 cells, sElk was stabilized at the non-permissive temperature (compare lanes 6 and 8), a further indication that the UPS participates in its degradation. As poly-ubiquitylation of Elk-1 in HEK293 cells and a temperature-dependent increase in the level of

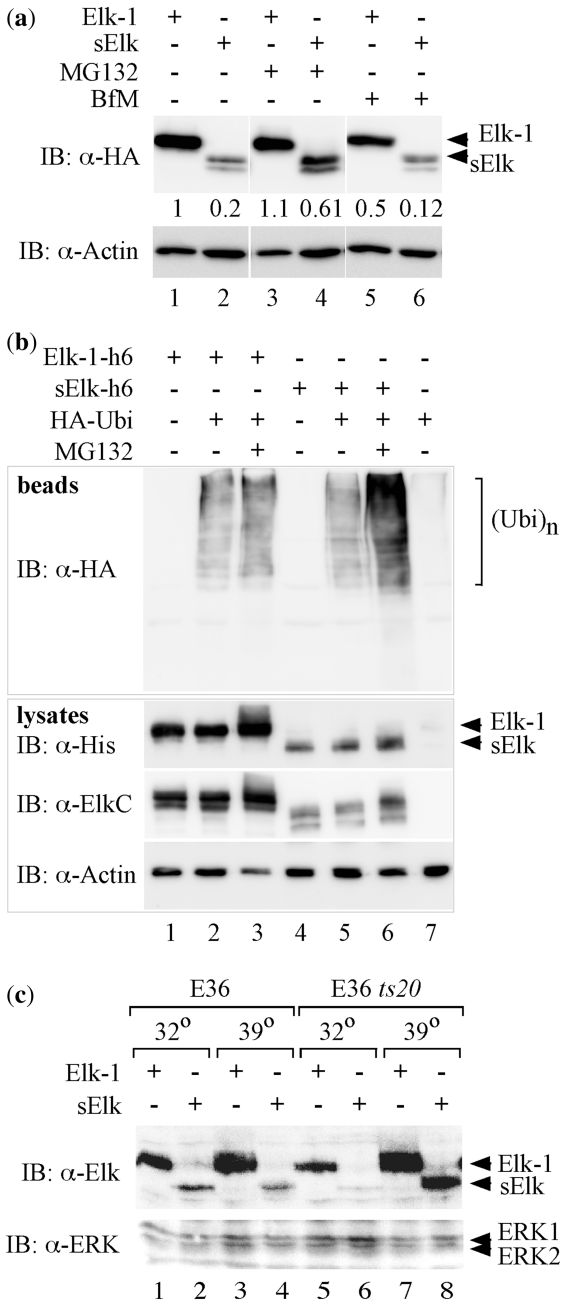

Figure 2. Removal of sElk by ubiquitin–proteasome system. (**a**) HEK293 cells were transfected with expression vectors for HA-tagged Elk-1 (lanes 1, 3 and 5) or sElk (lanes 2, 4 and 6). After 48 h lysates were prepared from untreated cells (lanes 1 and 2) or after treatment for 16 h with 20 μM MG132 (lanes 3 and 4) or 1 μM Bafilomycin (lanes 5 and 6) and examined by SDS–PAGE and immunoblotting. Numbers between panels indicate relative expression levels normalized to actin. (**b**) HEK293 cells were transfected with expression vectors for his-tagged Elk-1 (lanes 1–3) or sElk (lanes 4–6) and/or HA-tagged ubiquitin (lanes 2 and 3, 5–7). After 48 h lysates were prepared from untreated cells or after treatment with MG132 for 16 h (lanes 3 and 6) and subjected to IMAC. Eluates and lysates were subsequently examined by SDS–PAGE and immunoblotting. (**c**) E36 cells (lanes 1–4) or their *ts*20 derivative (lanes 5–8) were transfected with expression vectors for Elk-1 (lanes 1, 3, 5 and 7) or sElk (lanes 2, 4, 6 and 8). Cells were incubated at 32°C for 36 h or shifted to the non-permissive temperature (39°C) for 12 h prior to harvest. Cell lysates were prepared and Elk-1/sElk accumulation was monitored by SDS–PAGE and immunoblotting. Lower panel shows ERK re-probe as loading control.

Elk-1 in E36 *ts20* cells were also detected, we infer that Elk-1 is also turned over by the UPS, albeit less rapidly.

A short region of the ETS domain and a cryptic degron control Elk-1 accumulation

To define the region of the ETS domain required for Elk-1 accumulation, we first compared a series of short N-terminal truncations. Elk-1 lacking 6 or 16 amino-terminal amino acids, including helix α1, was stable (Figure 3a, lanes 1 and 2), but removal of a further eight residues (Δ1-24), including the adjacent α1β1 loop, had a clear destabilizing effect (lane 3) and deletions lacking 32 or 54 amino acids failed to accumulate (lanes 4 and 5; Figures 1 and 2). The effects of short internal deletions in the same region of the ETS domain were variable (Figure 3b and c). Deletions Δ7-16 and Δ13-20 had no effect whereas deletions Δ17-23 and Δ22-30 partially destabilized Elk-1 (Figure 3b, lanes 1, 3, 4 and 5). The internal deletion Δ9-24 severely destabilized Elk-1 (lane 2; Figure 3c). These internal deletions also implicate the α1β1 loop in the stability of Elk-1. As the ETS domain is responsible for DNA binding by Elk-1, we considered the possibility that the stability of the various mutants correlated with their ability to bind DNA. However, the only mutant with appreciable affinity for the c-*fos* SRE (in conjunction with SRF) was Elk-Δ1-6 (Supplementary Figure S2). In summary, a region of the ETS domain including amino acids 20–24 (Figure 3c) is crucial for the stability of Elk-1 in HEK293 cells and there is no correlation between DNA binding and stability.

Elk-1 is not quintessentially sensitive to deletions. When a series of internal deletion mutants throughout Elk-1 was generated (Figure 3d) and expressed in HEK293 cells they all accumulated to similar levels as full length Elk-1 (Figure 3e, odd lanes), suggesting that destabilization of Elk-1 was specific to N-terminal truncations. To see if Elk-1 contained a cryptic degradation signal activated by N-terminal truncation, the 32 N-terminal residues were removed from all the Elk-1 internal deletion mutants and accumulation of the double deletion mutants was compared (Figure 3e, even lanes). Only the double deletion mutant lacking amino acids 167–216 (Δ49, lane 6) accumulated significantly and reproducibly, suggesting that this deletion had compromised a degradation signal in Elk-1.

Rapid protein degradation has been attributed to the presence of 'PEST sequences' (rich in P, E, S and T residues) within target proteins. A web-based algorithm (PEST-FIND, EMBnet Austria) identified a single amino acid sequence in Elk-1 with a positive score (residues 197–230), which overlapped the Δ49 deletion (residues 167–216). However, a mutant with a shorter deletion (residues 167–196) that retained the predicted PEST motif was stable (Figure 3f and g, lane 4) and insertion of a heterologous 20 amino acid PEST motif from the human erythroid-specific transcription factor EKLF/KLF1 (25) in place of residues 167–216 also failed to destabilize the Elk-Δ1-32/Δ49 double deletion (lane 6). In contrast, when residues 187–216 were deleted, the double deletion was again de-stabilized

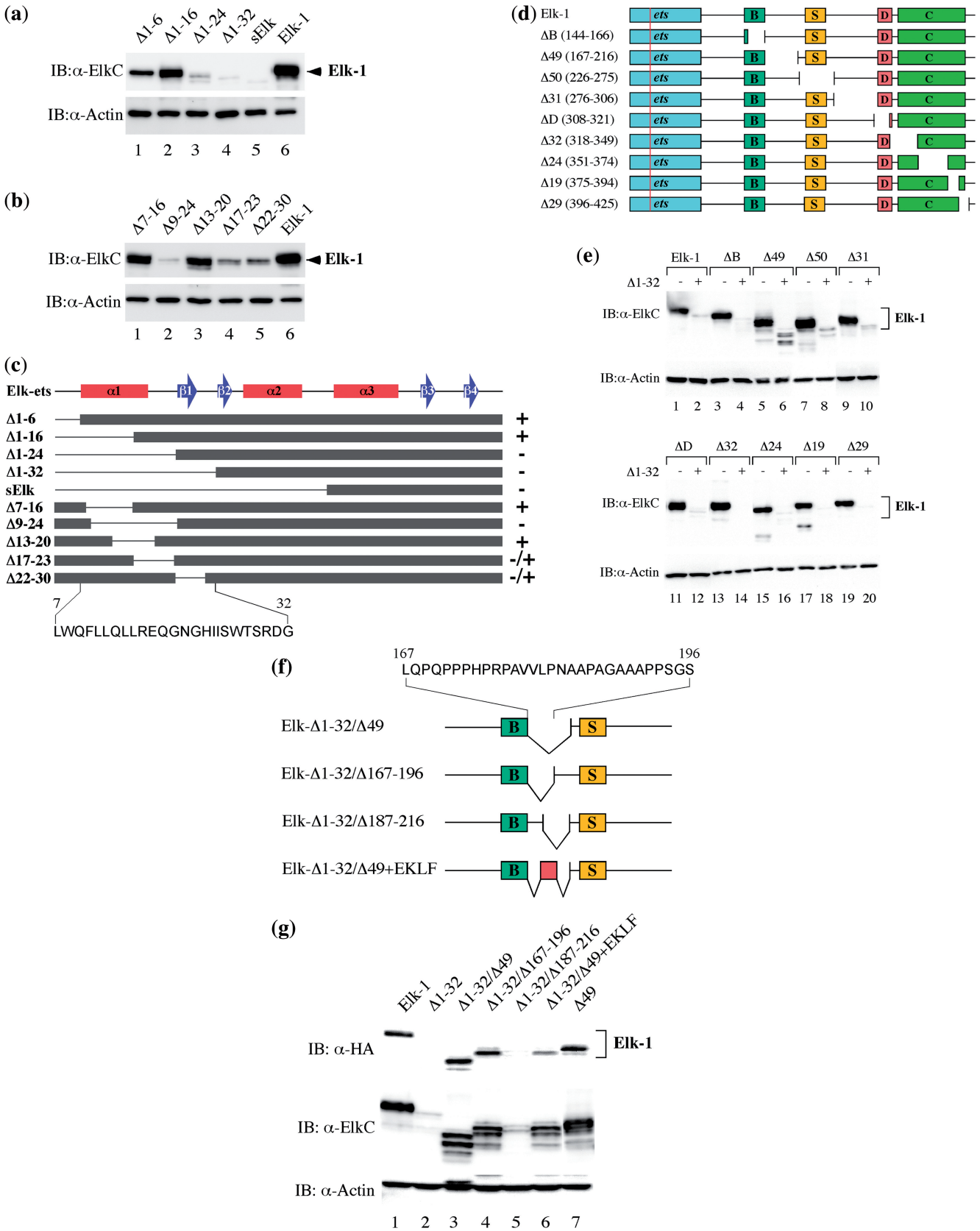

Figure 3. Elk-1 harbours a stability motif and a cryptic degradation signal. (**a**) HEK293 cells were transfected with expression vectors for Elk-1 and the amino-terminal truncations indicated. Cell lysates were prepared and Elk-1 expression monitored by SDS–PAGE and immunoblotting. Lower panel shows actin re-probe as loading control. (**b**) As in (a) except cells were transfected with expression vectors for Elk-1 and the internal deletions indicated. (**c**) Diagram of Elk-1 amino-terminal truncation and internal deletion mutants aligned with respect to the ETS domain

(continued)

(Figure 3g, compare lane 5 with lanes 3 and 4). From these data, we conclude that a proline-rich hydrophobic motif (PRM) adjacent to the SID (Figure 3f) serves as a cryptic degron to drive the turnover of destabilized N-terminal truncations of Elk-1.

Elk-1 stability correlates with dimer formation

The activation of a cryptic degron within the body of Elk-1 by short deletions in the ETS domain suggested a significant change in protein conformation. Having previously reported that Elk-1 forms dimers and that dimerization might involve the ETS domain (5) we next assessed the contribution of the ETS domain to dimer formation. First we compared recombinant Elk-1 and sElk proteins in gel filtration experiments. Full length Elk-1 ran as a 120–140 kDa species as previously reported (5), regardless of whether it was purified under native or denaturing conditions and subsequently renatured (Supplementary Figure S3a). In contrast, sElk ran at 40–60 kDa close to its monomer mass (Figure 4a). In a low salt buffer (50 mM KCl) the recombinant ETS domain of Elk-1 (Elk-ets) ran predominantly as a peak above 17 kDa, but in 250 mM KCl the peak shifted to below 17 kDa (Figure 4b), implying that formation of ETS domain dimers is salt sensitive. To confirm dimerization by the Elk-1 ETS domain, gel filtration profiles of Elk-1, Elk-ets and mixtures of the two were compared. Individually both proteins ran as dimers but with some monomer apparent (Figure 4c, lower panels). Importantly, in the mixture with Elk-1 a second peak of Elk-ets appeared at around 100 kDa, indicative of heterodimers between Elk-ets and full length Elk-1.

As a further test for ETS domain dimerization and to see if the region encompassing the $\alpha1\beta1$ loop was involved in the interaction, we performed GST pull-down experiments with Elk-ets and the Δ17-23 deletion mutant expressed as GST-fusions (Supplementary Figure S3b) and with HA tags. HA-Elk-ets and HA-Elk-etsΔ17-23 (Δ17-23) both interacted with immobilized GST-Elk-ets (Figure 4d, lanes 3 and 4). HA-Elk-ets also interacted with GST-etsΔ17-23 (lane 5) but HA-Elk-etsΔ17-23 did not (lane 6). From this we infer that the Elk-ets domain is able to homo-dimerize, consistent with the findings of the gel filtration experiments. The Δ17-23 mutant is unable to self-dimerize, but is still able to interact with the intact Elk-1 ETS domain. This hetero-dimerization would explain the intermediate stability observed for the Δ17-23 mutant in HEK293 cells (Figure 3b) where it could dimerize with endogenous Elk-1.

Elk-1 dimers are restricted to the cytoplasm

To assess dimer formation by Elk-1 in living cells we used BiFC with fragments of a red-shifted version of GFP [Venus-yellow fluorescent protein (YFP)] (26,27) fused to the carboxy-terminus of Elk-1. Expression of an analogous Elk-GFP fusion confirmed that Elk-1 was predominantly, but not exclusively nuclear in HeLa cells (Figure 5a) (9). Elk-1 fusions with YFP moieties alone gave no fluorescence [Figure 5b(i) and (ii)]. Co-expression with the reciprocal, YFP moieties alone yielded background fluorescence complementation throughout the cells [Figure 5(iii) and (iv)]. Co-expression of the complementary Elk-1-YFP fusions gave a strong fluorescent signal indicative of Elk-1 dimer formation [Figure 5b(v)]. This signal was distributed throughout the cytoplasm but was absent from the nucleus. Expression of Elk-1 fusions with YFPn and YFPc fragments was confirmed by immunoblotting with an anti-Elk-1 antibody, and cell fractionation indicated that both fusions were present in cytoplasm and nucleus (Figure 5c).

When the Δ9-24 deletion (Figure 3c) was introduced into the Elk-YFP fusions, fluorescence complementation was lost, which could be explained simply by rapid degradation of the two proteins. However, when cells were treated with MG132, fluorescence complementation was still not detected even though the fusion proteins were present (Supplementary Figure S4a and b), indicating that ETS domain dimerization is required for efficient YFP complementation.

Complementation by the YFP moieties is irreversible so the absence of nuclear fluorescence indicates that the cytoplasmic Elk-1 dimers captured by BiFC do not enter the nucleus. In addition, the presence of both Elk-YFP fusions together in the nucleus (Figure 5c, lower panel, lane 5) suggests that one or more factors preclude Elk-1 dimer formation within the nucleus. Elk-1 may not be typical of ETS domain proteins as two other ETS proteins, Ets-1 and PU.1 (Spi I), both promoted strong nuclear complementation (Figure 5d), confirming that BiFC can take place in the nucleus and consistent with the notion that other ETS proteins form dimers (28).

Dimerization and DNA binding by the Elk-1 ets domain are mutually exclusive

The crystal structure of the DNA-bound Elk-1 ETS domain [1DUX] (29) implies that DNA binding by an ETS domain dimer is possible, whereas the absence of nuclear BiFC suggests that Elk-1 dimers are not present in the nucleus. When a radio-labelled ETS consensus site

Figure 3. Continued
structure (top), in which helices are indicated by red boxes and strands by blue arrows. For each mutant, lines indicate regions deleted and instability/stability (−/+) is indicated to the right. The sequence of the region implicated in dimer formation is shown below. (**d**) Diagram of Elk-1 internal deletion mutants generated with or without partial deletion of amino-terminal ETS domain (residues 1–32), as indicated by vertical red line. Domains are B: SRF-interaction; S: repression; D: MAPK docking; C: trans-activation. Residues lost in each internal deletion are given in parentheses. (**e**) HEK293 cells were transfected with expression vectors for Elk-1 and the indicated deletion mutants without (−) or with (+) the additional deletion of residues 1–32. After 48 h whole cell lysates were prepared and Elk-1 expression monitored by SDS–PAGE and immunoblotting. Lower panel shows actin re-probes as loading control. (**f**) Diagram of Elk-1 double deletion mutants derived from Elk-Δ1-32/Δ49 including insertion of a PEST sequence from EKLF (red box). The sequence harbouring the cryptic degron is shown above. (**g**) HEK293 cells were transfected with expression vectors for Elk-1 (lane 1), ElkΔ1-32 (lane 2), Elk-Δ1-32/Δ49 (lane 3), Elk-Δ1-32/Δ167-196 (lane 4), Elk-Δ1-32/Δ187-216 (lane 5) Elk-Δ1-32/Δ49+EKLF (lane 6) or Elk-Δ49 (lane 7) and processed as described in (e).

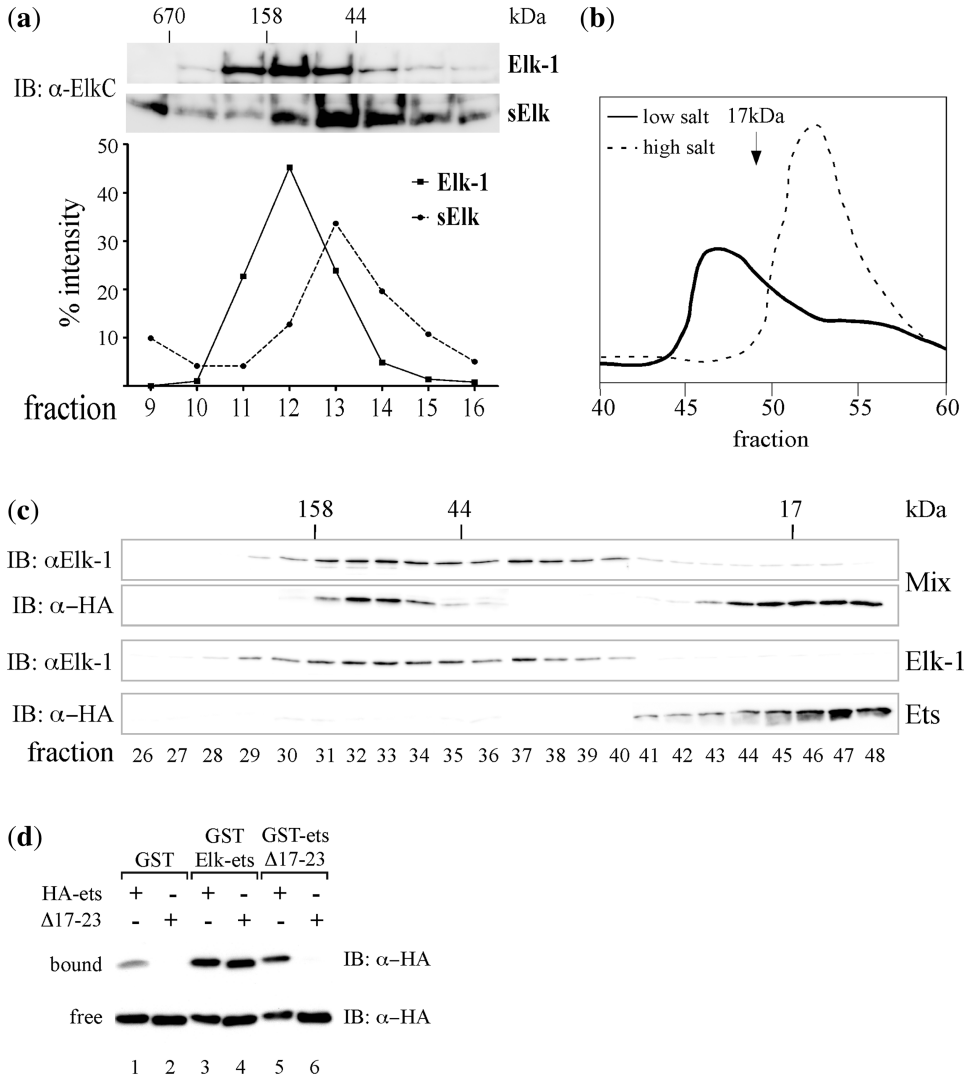

Figure 4. Elk-ets domain mediates Elk-1 dimer formation. (**a**) Recombinant Elk-1 and sElk were purified by IMAC and analysed by gel filtration followed by SDS–PAGE and immunoblotting of fractions. Graph shows intensity (%) of bands measured by digital image analysis (Aida). (**b**) Recombinant Elk-ets purified by IMAC was analysed by gel filtration in buffers containing 50 mM (low) and 250 mM (high) KCl. Traces show UV absorption. (**c**) Elk-1 and Elk-ets both as individual proteins and mixed as described in methods were analysed by gel filtration followed by SDS–PAGE and immunoblotting of fractions. (**d**) Recombinant HA-Elk-ets (lanes 1, 3 and 5) or HA-Elk-etsΔ17-23 (lanes 2, 4 and 6) were incubated with immobilised GST (lanes 1 and 2) GST-Elk-ets (lanes 3 and 4) or GST-Elk-etsΔ17-23 (lanes 5 and 6). Bound and free fractions were detected by SDS–PAGE and immunoblotting.

(E74 duplex) was incubated with Elk-ets (1 ng) and analysed by EMSA, a single complex was observed (Figure 6a, lane 2), and a 25-fold increase in protein yielded no additional complexes (lanes 3–7). The Elk-ets complex could represent either a monomer or a dimer bound to DNA. However, when we co-incubated Elk-ets and Elk-ΔA (residues 1–253) with E74 DNA, no intermediate complex was detected (Figure 6b, lane 2), indicating that both proteins bind DNA as monomers. As PU.1 formed nuclear dimers detectable by BiFC (Figure 5d) we also compared DNA binding by the PU.1 ETS domain (PU.1-ets) and Elk-ets. PU.1-ets bound to E74 DNA but the complex migrated significantly slower than the Elk-ets complex (Figure 6b, lanes 4 and 6), suggesting that PU.1 might bind to DNA as a dimer.

DNA binding experiments were also performed with ETS domains and unlabelled DNA, in which complexes in native gels were visualized with coomassie blue. Elk-ets alone did not enter the gel (Figure 6c, lane 3) but after incubation with E74 DNA gave rise to a discrete complex corresponding to an Elk-ets monomer bound to the E74 duplex (lane 4). Incubation with a control DNA duplex lacking an ETS binding motif gave no complex (lane 5). Ethidium bromide staining of the gel revealed retarded migration of E74 but not control DNA, confirming the interaction with Elk-ets. An Elk-ets mutant (R65A, Y66F) defective for DNA binding (ets-DM; Supplementary Figure S5) failed to interact with E74 DNA (lane 7). PU.1-ets also interacted with E74 DNA in this system (lane 9), forming

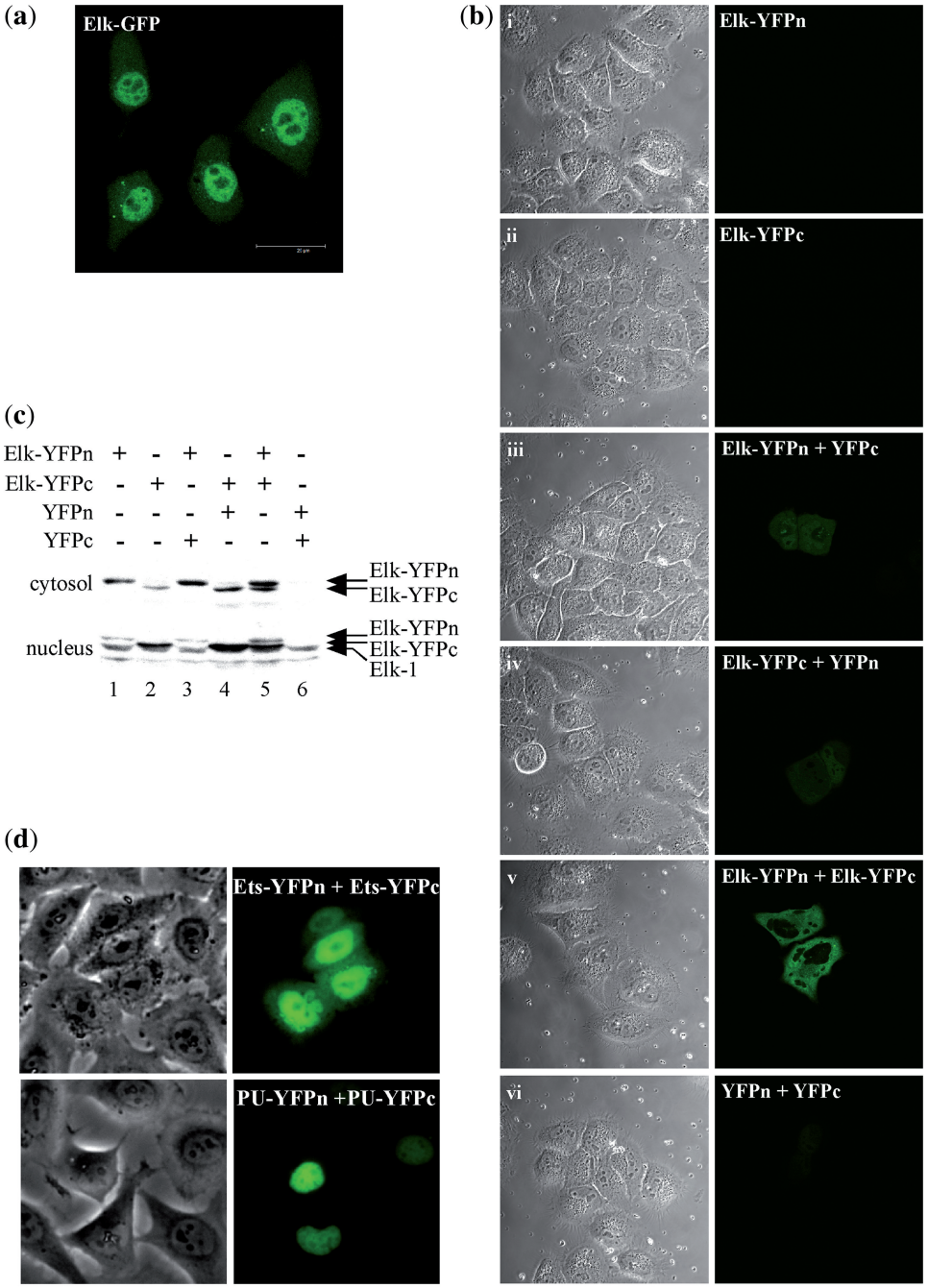

Figure 5. Elk-1 dimers are restricted to the cytoplasm. (**a**) HeLa cells transfected with an expression vector for Elk-GFP were imaged by confocal microscopy. Scale bar is 25 μm. (**b**) Differential interference contrast (DIC) and confocal images of live HeLa cells 16 h post-transfection with Elk-YFPn (i), Elk-YFPc (ii), Elk-YFPn with YFPc (iii), Elk-YFPc with YFPn (iv), Elk-YFPn with Elk-YFPc (v) and YFPn with YFPc (vi). (**c**) HeLa cells were transfected with expression vectors for Elk-YFPn (lanes 1, 3 and 5), Elk-YFPc (lanes 2, 4 and 5), YFPn (lanes 4 and 6) and/or YFPc (lanes 3 and 6). After 24 h cells were harvested, nuclear and cytoplasmic fractions were prepared, separated by SDS–PAGE and analysed by immunoblotting with an antibody against Elk-1. (**d**) Phase contrast and fluorescence images of live HeLa cells 16 h post transfection with Ets-1-YFPn with Ets-1-YFPc (upper) and PU.1-YFPn with PU.1YFPc (lower panels).

a complex that migrated more slowly than the Elk-ets complex, but too fast for a PU.1-ets dimer. Its slower migration may reflect the slightly higher MW and number of basic residues in the PU.1-ets domain. Thus, although BiFC detected nuclear PU.1 dimers, both Elk-1 and PU.1 ETS domains bind to DNA as monomers. We therefore tested the effect of DNA on Elk-ets dimers in GST pull-down assays. Pre-incubation with E74 DNA blocked the interaction between Elk-ets domains whereas DNA lacking an ETS motif did not (Figure 6d). Together these data indicate that Elk-1 and Elk-ets bind to DNA as monomers and that ETS domain dimerization and DNA binding in solution may be mutually exclusive.

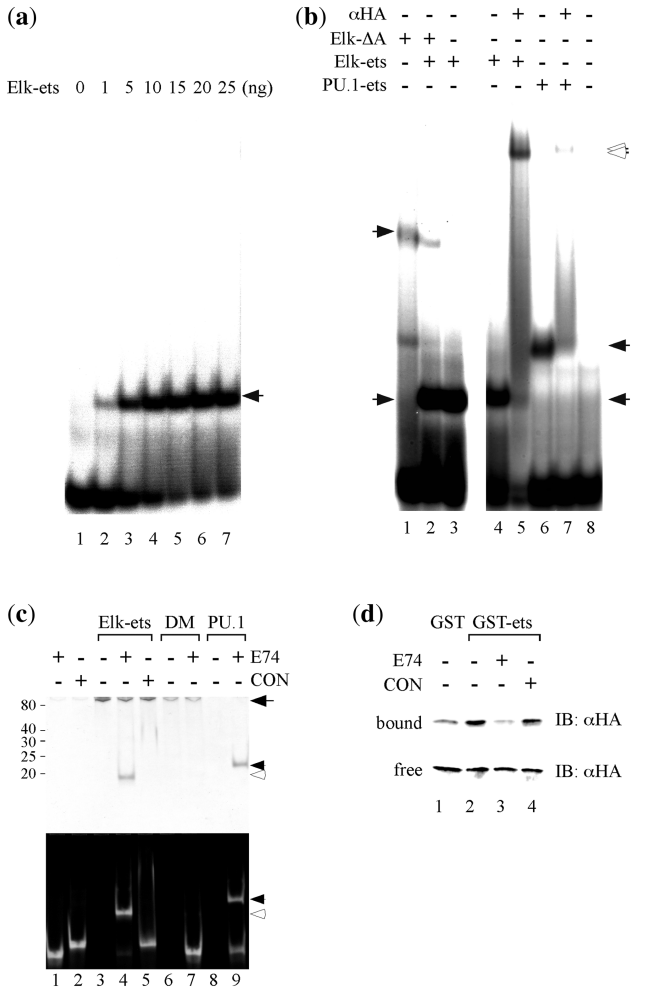

Figure 6. Elk-ets domain binds DNA as a monomer. (**a**) Radio-labelled E74 probe was incubated alone (lane 1) or with increasing amounts of recombinant HA-tagged Elk-ets (1–25 ng) and complexes were resolved by EMSA. (**b**) Elk-ΔA (residues 1–253; 10 ng) and HA-Elk-ets (10 ng) were incubated alone (lanes 1 and 3, respectively) or together (lane 2) with radio-labelled E74 DNA. Similarly 10 ng each of HA-Elk-ets (lanes 4 and 5) or HA-PU.1-ets (lanes 6 and 7) were incubated in the absence (lanes 4 and 6) or presence (lanes 5 and 7) of anti-HA antibody and E74 DNA. Complexes were resolved by EMSA. Filled arrowheads indicate complexes and open arrowheads indicate supershifts. (**c**) About 60 pmol of E74 duplex (29 bp) was incubated alone (lane 1) or with 1 μg HA-Elk-ets (lane 4), HA-ets-DM (lane 7) and HA-PU.1-ets (lane 9), and 60 pmoles of control duplex (CON; 33 bp) was incubated alone (lane 2) or with 1 μg HA-Elk-ets (lane 5) for 10 min at RT before resolution on a 12% non-denaturing polyacrylamide gel. The gel was stained first with ethidium bromide (lower panel) and subsequently with coomassie blue. Arrow indicates unbound protein; open arrowhead indicates Elk-ets/E74 complex; filled arrowhead indicates PU.1-ets complex. (**d**) Recombinant HA-Elk-ets was incubated with immobilized GST (lane 1) or GST-Elk-ets (lanes 2–4) in the absence (lane 2) or presence of specific E74 (lane 3) or non-specific control DNA (CON) (lane 4). Bound and free fractions were detected by SDS–PAGE and immunoblotting.

DNA interactions contribute to nuclear retention of Elk-1

The ability of DNA to dissociate Elk-1 dimers *in vitro* implied that DNA binding could contribute to the absence of nuclear Elk-1 dimers. To explore this further, we measured the proportion of DNA-bound Elk-1 in HeLa nuclei by fluorescence recovery after photobleaching (FRAP). Recovery by Elk-GFP was complete within 2.5 s (Figure 7a, upper panel), indicating that nuclear Elk-1 is highly mobile. The same profile was observed with a DNA binding-defective Elk-1 mutant (Elk-DM) (Figure 7a, lower panel), indicating that there is little or no immobile Elk-1 fraction bound stably to DNA. This result is inconsistent with stable binding of Elk-1 in SRE promoter complexes and implies dynamic DNA interactions, although theoretically, stably bound, endogenous Elk-1 could have excluded Elk-GFP from the DNA. However, upon cell fractionation we observed that whereas Elk-1 and Elk-SM, a mutant unable to interact with SRF, were predominantly nuclear, Elk-DM had an altered cellular distribution that was largely cytoplasmic (Figure 7b).

To follow the flux of Elk-1 between cytoplasm and nucleus we used fluorescence loss in photobleaching (FLIP). For Elk-1 and Elk-SM no redistribution between compartments was apparent over 1 h, whereas movement of Elk-DM in and out of the nucleus was readily detected (Figures 7c). These data indicate that Elk-1 is highly mobile in the nucleus yet undergoes dynamic interactions with DNA that contribute to its nuclear accumulation. Nonetheless, the DNA binding-defective Elk-1 mutant (Elk-DM) did not form nuclear dimers (Figure 7d), even when nuclear export was inhibited (Supplementary Figure S6). From these data we conclude that although DNA interactions may aid nuclear accumulation they do not account for the absence of nuclear Elk-1 dimers.

DISCUSSION

Cells use a range of mechanisms to constrain transcriptional activators until they are required, including inhibitory conformations or complexes, the need for activating post-translational modification and, in some instances, the self-limiting coupling of activator function to protein degradation. Here we have revealed novel features of Elk-1 that determine its native conformation, its stability in the cytoplasm of cells and its nuclear accumulation as a latent transcription factor.

Factors determining the cytoplasmic instability of Elk-1

Protein quality control systems exist in eukaryotic cells to recognize mis-folded proteins, which can either be refolded correctly or degraded to prevent their aggregation with potentially disastrous consequences (19,20). Two motifs in Elk-1 determine its premature degradation: a region of the ETS domain encompassing the α1β1 loop distal to the DNA-binding α3 helix, and a second motif in the body of Elk-1 mapped by internal deletions to a PRM adjacent to the SID. Although ETS domains are well conserved overall, residues encompassing the α1β1 loop are not. This could imply that dimerization by ETS proteins is specific and selective; equally it could indicate promiscuity. The PRM is not conserved among ternary complex factors (TCFs) and has no obvious counterpart in other ETS proteins. It also bears little resemblance to PEST sequences and a weak PEST

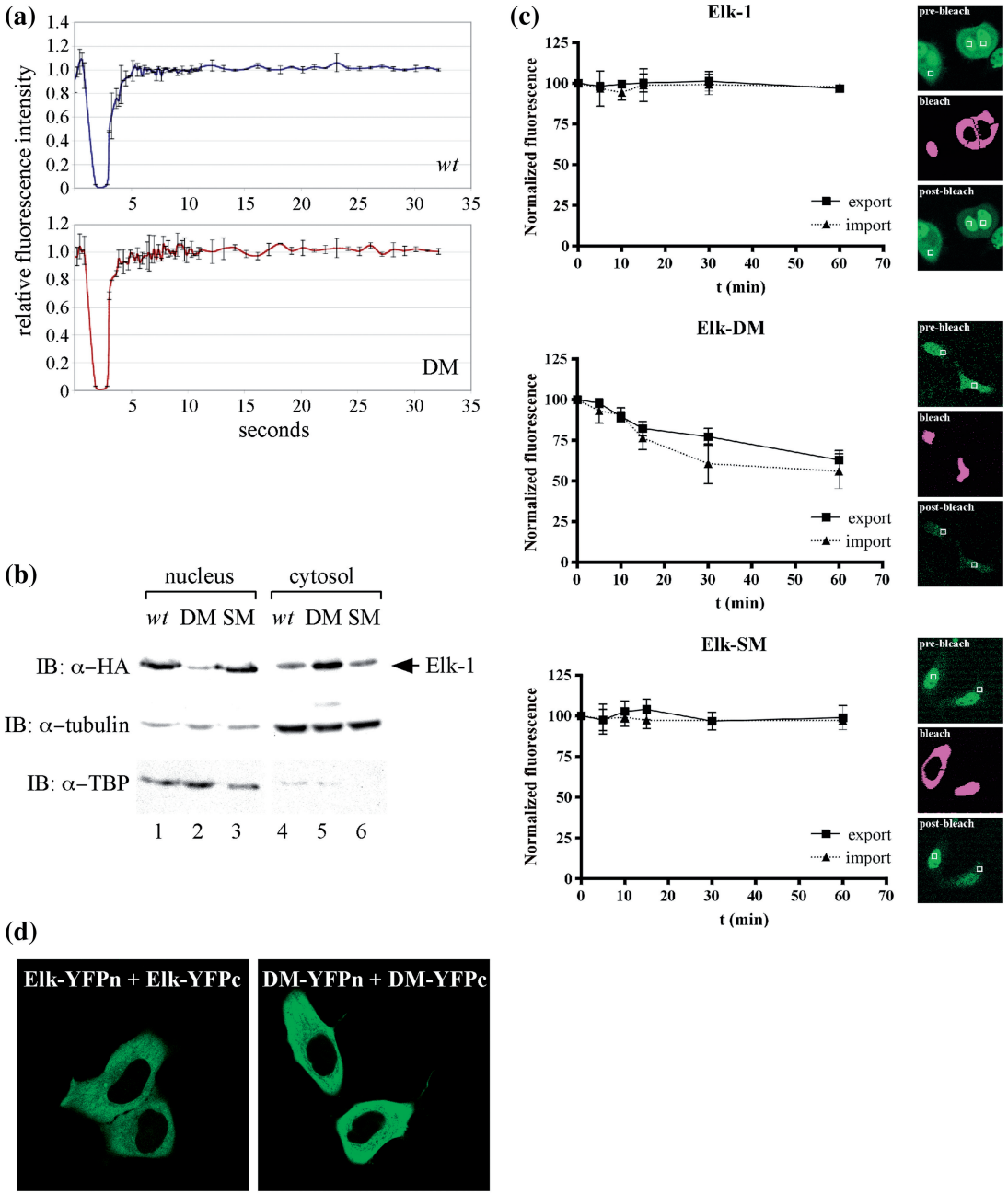

Figure 7. Mobility and accumulation of Elk-1 in HeLa nuclei. (**a**) HeLa cells cultured in glass-bottomed petri dishes were transfected with vectors for Elk-GFP or Elk-DM-GFP and after recovery for 24 h in full medium, mobility of Elk-1 was determined by FRAP. Data presented are average values (−/+ SE) for recovery measured on 10 individual cells from one representative experiment. (**b**) Nuclear and cytosolic fractions were prepared from HEK293 cells transfected with expression vectors for Elk-1 (lanes 1 and 4) Elk-DM (lanes 2 and 5) and Elk-SM (lanes 3 and 6) were separated by SDS–PAGE and analysed by imunoblotting with the antibodies indicated. (**c**) HeLa cells cultured in glass-bottomed petri dishes were transfected with vectors for Elk-GFP, Elk-DM-GFP or Elk-SM-GFP and after recovery for 24 h in full medium, mobility of Elk-1 was followed by FLIP over 60 min. Data are compiled from measurements on five individual cells for each time course (error bars show SEM). Panels show examples of cells prior to bleach (upper), immediately after bleach (middle) and 60 min post bleach (lower). (**d**) Fluorescence images of live HeLa cells 16 h post-transfection with expression vectors for Elk-YFPn and Elk-YFPc (left panel) or Elk-DM-YFPn and Elk-DM-YFPc (right).

consensus further downstream played no role in destabilizing Elk-1. This was confirmed by the introduction of a well-defined PEST motif derived from EKLF (25), which had only a slight destabilizing effect on N-terminal Elk-1 truncations.

Exposed hydrophobic patches are known to provide recognition motifs for chaperones involved in protein quality control (30). For example, the activity of Hsc70 is coordinated by several co-chaperones including CHIP (carboxy-terminus of Hsc70-interacting protein), a chaperone-dependent ubiquitin E3 ligase that poly-ubiquitylates mis-folded proteins (31). Indeed, in association with BAG-1, an ubiquitin domain protein, the Hsc70/CHIP complex can direct proteasomal

degradation of proteins independent of their ubiquitylation (32).

Although the destabilizing function of the PRM is countermanded by an N-terminal region of the ETS domain, the two motifs are unlikely to interact directly. ETS domain dimerization more likely promotes folding of the remainder of Elk-1 to mask the PRM, thereby preventing degradation. As such dimerization would effectively serve as a quality control mechanism for the intact DNA binding domain, preventing a potentially rogue trans-activation domain from reaching the nucleus and undergoing non-productive interactions with transcriptional co-activators. A precedent for the stabilization of transcription factor dimers is seen with C/EBPδ, in which the leucine zipper serves as the dimer interface (33). Although altered protein expression levels may influence localization, DNA binding and degradation, the use of vectors that express Elk-1 above endogenous levels underlines the capacity of cells to remove mutants defective for dimerization. It will be of interest to determine the consequences of mutating the PRM in full length Elk-1.

Implicit in the accumulation of sElk in neuronal cells is that stability can be achieved without ETS domain-mediated dimerization. In this scenario the PRM may be masked by other molecular interactions or its recognition sensor may be absent from those neuronal cells in which sElk is stable. The detection of poly-ubiquitylated sElk and the stabilization of sElk by MG132 or inactivation of a temperature-sensitive E1 enzyme are consistent with the PRM serving as the recognition element for an E3 ubiquitin ligase, although at present we cannot rule out a contribution by other pathways. Besides chaperone-mediated degradation, other potential ubiquitin-independent pathways include 'degradation by default', which has been proposed for inherently unstable proteins, and chaperone-mediated autophagy (34,35). As Bafilomycin, a V-ATPase inhibitor that prevents maturation of autophagic vacuoles, did not stabilize sElk, we infer that truncated Elk-1 proteins are not removed by autophagy.

Allosteric control of DNA binding by ETS domains

Despite earlier reports (3,28), dimerization is a phenomenon not generally associated with ETS proteins. In the case of TEL (ETV6), the pointed (PNT) domain, which is shared by a sub-group of ETS proteins, has been implicated in multimerization and repression whereas in Ets-1 the domain is monomeric and aids trans-activation by virtue of an integral MAPK docking site (36,37). The ETS domain of GABPα forms heterodimers with GABPβ, stabilized by a carboxy-terminal α-helical extension to the ETS domain that aligns with several ankyrin repeats in GABPβ (38). This α-helical extension bears analogy to the auto-inhibitory domain of Ets-1, which consists of a pair of helices to either side of the ETS domain that associate with the α1 helix, reducing DNA affinity 20-fold by changing the structure of the domain and the ability of loops at either end of the α3 recognition helix to interact with DNA (39).

The capacity to influence DNA binding by altering molecular interactions distal to the recognition helix within ETS domains was recognized earlier in Sap1a and Elk-1 (29,40). Auto-inhibitory domains are also present in the TCFs Net and Sap1a, but notably not in Elk-1 (41,42). They form inhibitory complexes with ETS domains and are proposed to operate in *cis*, although action *in trans* has not been ruled out. The helix-loop-helix (HLH) structure of these inhibitory domains is shared with Id proteins, which have also been shown to interact with TCFs and prevent DNA binding (43), although the exact nature of the binding interface has not been resolved. Interactions between winged helix domains involving the end of α1 and adjacent loops are evident in ESCRT complexes engaged in protein sorting (44). It is therefore conceivable that inhibition of ETS domain proteins by HLH domains involves a similar interface as ETS domain dimerization in Elk-1.

The data herein demonstrating a role for Elk-1 dimerization have extended earlier work substantially (3). The initial, indirect mapping of the interface through protein stability was confirmed by biochemical interaction studies. The ability of the Δ17-23 mutant to dimerize with the intact Elk-ets domain *in vitro* was unanticipated but offered an explanation for its partial stability in cells. Also unexpected was the localization of Elk-1 dimers to the cytoplasm. Interpretation of BiFC data can be limited by factors such as temperature sensitivity and irreversibility (26), but the use of early time points post-transfection and inclusion of multiple controls strengthened our interpretation that efficient complementation required Elk-1 dimer formation. A further advantage of this BiFC analysis was that it highlighted the sub-population of Elk-1 dimers in contrast to the bulk of Elk-1 illuminated by Elk-GFP.

DNA binding and nuclear accumulation of Elk-1 monomers

At least two factors contribute to the absence of nuclear Elk-1 dimers. Firstly the nuclear import mechanism, which for other ETS proteins has been shown to involve importin-mediated recognition of NLS motifs overlapping key residues in DNA binding (45), appears likely, for this reason, to separate dimers. Secondly, as both Elk-YFP fusions reach the nucleus and nuclear YFP complementation clearly occurs (Figure 5d) (26), Elk-1 must be prevented from re-forming dimers once in the nucleus. Although DNA binding inhibited Elk-1 dimer formation *in vitro*, the notion that DNA binding might serve to inhibit nuclear dimerization could not be substantiated. Indeed, FRAP analyses highlighted the mobility of nuclear Elk-1 and the likely absence of a stable DNA-bound fraction. However, complementary FLIP experiments revealed a significant re-localization of Elk-DM from nucleus to cytoplasm, implying that ongoing dynamic DNA-interactions by Elk-1 contribute to its nuclear retention. Although we cannot entirely rule out that the mutations in Elk-DM (R65A, Y66F) alter nuclear import or export of Elk-1 directly, we have observed a similar cytoplasmic redistribution of other,

but not all, DNA binding defective Elk-1 proteins (data not shown). These observations draw into question interpretations of static imaging data that have mapped NLS motifs within DNA binding helices of ETS proteins, as import and retention may not have been distinguished. That aside, it appears that interactions with other factors, for example HLH domain proteins, may serve to out-compete Elk-1 dimer formation in the nucleus.

The FRAP and FLIP data presented here suggest that DNA interactions by Elk-1 contribute significantly to its nuclear accumulation, but at the same time they are dynamic and, crucially, have little impact on nuclear mobility (46). From this it follows that the number of ETS binding sites available within the genome (or heterochromatin) could determine nuclear levels of Elk-1 (and other ETS proteins) with excess molecules re-exported to the cytoplasm either to dimerize or become degraded. This model also implies that the concentration of Elk-1 could vary between sub-nuclear regions as a function of the genomic distribution of ETS binding sites and the nuclear architecture. A prediction of the model would be the clustering of consensus ETS binding sites near the 5′-ends of target genes to ensure working concentrations of Elk-1 at responsive promoters, which is what has been observed (47). On the basis of the findings reported here, it will be interesting to establish the nature and chronology of events propelling latent Elk-1 towards the establishment of active promoter complexes at mitogen-responsive genes.

SUPPLEMENTARY DATA

Supplementary Data are available at NAR Online.

ACKNOWLEDGEMENTS

We thank Guillaume Bossis (Montpellier) for the E36 cell lines, Paco Ciruela (Barcelona) for YFP BiFC vectors, Angie Rizzino (Nebraska) for Ets-1 and PU.1 cDNAs, Tim Self for confocal imaging, Martin Bushell for guidance on polysome fractionations, Ed Bolt for help with the gel filtration, Jerusalem Alleyne, Nicola Ambler, Ross Nieuburg and Petra Spangenberg for plasmid constructs, Thomas Strahl and Uwe Vinkemeier for discussions and Wendy Solis for secretarial assistance.

FUNDING

This work was funded by grants to PES from the BBSRC (refs C19717 and BB/D019117/1) and to RAH from the Association pour la Recherche sur le Cancer (No. 3967). Funding for open access charge: University of Nottingham.

Conflict of interest statement. None declared.

REFERENCES

1. Shaw,P.E. and Saxton,J. (2003) Ternary complex factors: prime nuclear targets for mitogen-activated protein kinases. *Int. J. Biochem. Cell Biol.*, **35**, 1210–1226.
2. Buchwalter,G., Gross,C. and Wasylyk,B. (2004) Ets ternary complex transcription factors. *Gene*, **324**, 1–14.
3. Drewett,V., Muller,S., Goodall,J. and Shaw,P.E. (2000) Dimer formation by ternary complex factor Elk-1. *J. Biol. Chem.*, **275**, 1757–1762.
4. Yang,S.-H., Shore,P., Willingham,N., Lakey,J.H. and Sharrocks,A.D. (1999) The mechanism of phosphorylation-inducible activation of the ETS-domain transcription factor Elk-1. *EMBO J.*, **18**, 5666–5674.
5. Drewett,V., Molina,H., Millar,A., Muller,S., von Hesler,F. and Shaw,P.E. (2001) DNA-bound transcription factor complexes analysed by mass-spectrometry: binding of novel proteins to the human c-*fos* SRE and related sequences. *Nucleic Acids Res.*, **29**, 479–487.
6. Yang,S.H. and Sharrocks,A.D. (2005) PIASx acts as an Elk-1 coactivator by facilitating derepression. *EMBO J.*, **24**, 2161–2171.
7. Heun,P. (2007) SUMOrganization of the nucleus. *Curr. Opin. Cell Biol.*, **19**, 350–355.
8. O'Donnell,A., Yang,S.H. and Sharrocks,A.D. (2008) MAP kinase-mediated c-fos regulation relies on a histone acetylation relay switch. *Mol. Cell*, **29**, 780–785.
9. Zhang,H.M., Li,L., Papadopoulou,N., Hodgson,G., Evans,E., Galbraith,M., Dear,M., Vougier,S., Saxton,J. and Shaw,P.E. (2008) Mitogen-induced recruitment of ERK and MSK to SRE promoter complexes by ternary complex factor Elk-1. *Nucleic Acids Res.*, **36**, 2594–2607.
10. Stevens,J.L., Cantin,G.T., Wang,G., Shevchenko,A. and Berk,A.J. (2002) Transcription control by E1A and MAP kinase pathway via Sur2 mediator subunit. *Science*, **296**, 755–758.
11. Reid,G., Hubner,M.R., Metivier,R., Brand,H., Denger,S., Manu,D., Beaudouin,J., Ellenberg,J. and Gannon,F. (2003) Cyclic, proteasome-mediated turnover of unliganded and liganded ERalpha on responsive promoters is an integral feature of estrogen signaling. *Mol. Cell*, **11**, 695–707.
12. Metivier,R., Penot,G., Hubner,M., Reid,G., Brand,H., Kos,M. and Gannon,F. (2003) Estrogen receptor-alpha directs ordered, cyclical, and combinatorial recruitment of cofactors on a natural target promoter. *Cell*, **115**, 751–763.
13. Sadowski,H.B. and Gilman,M.Z. (1993) Cell-free activation of a DNA-binding protein by epidermal growth factor. *Nature*, **362**, 79–83.
14. Johannes,G., Carter,M.S., Eisen,M.B., Brown,P.O. and Sarnow,P. (1999) Identification of eukaryotic mRNAs that are translated at reduced cap binding complex eIF4F concentrations using a cDNA microarray. *Proc. Natl Acad. Sci. USA*, **96**, 13118–13123.
15. Gille,H., Sharrocks,A.D. and Shaw,P.E. (1992) Phosphorylation of transcription factor p62TCF by MAP kinase stimulates ternary complex formation at c-fos promoter. *Nature*, **358**, 414–417.
16. Gille,H., Kortenjann,M., Thomae,O., Moomaw,C., Slaughter,C., Cobb,M.H. and Shaw,P.E. (1995) ERK phosphorylation potentiates ELK-1-mediated ternary complex formation and transactivation. *EMBO J.*, **14**, 951–962.
17. Gille,H., Kortenjann,M., Strahl,T. and Shaw,P.E. (1996) Phosphorylation-dependent formation of a quaternary complex at the c-fos SRE. *Mol. Cell. Biol.*, **16**, 1094–1102.
18. Araud,T., Genolet,R., Jaquier-Gubler,P. and Curran,J. (2007) Alternatively spliced isoforms of the human elk-1 mRNA within the 5' UTR: implications for ELK-1 expression. *Nucleic Acids Res.*, **35**, 4649–4663.
19. Hartl,F.U. and Hayer-Hartl,M. (2002) Molecular chaperones in the cytosol: from nascent chain to folded protein. *Science*, **295**, 1852–1858.
20. Broadley,S.A. and Hartl,F.U. (2009) The role of molecular chaperones in human misfolding diseases. *FEBS Lett.*, **583**, 2647–2653.
21. Hassler,M. and Richmond,T.J. (2001) The B-box dominates SAP-1-SRF interactions in the structure of the ternary complex. *EMBO J.*, **20**, 3018–3028.
22. Mo,Y., Ho,W., Johnston,K. and Marmorstein,R. (2001) Crystal structure of a ternary SAP-1/SRF/c-*fos* SRE complex. *J. Mol. Biol.*, **314**, 495–506.
23. Welchman,R.L., Gordon,C. and Mayer,R.J. (2005) Ubiquitin and ubiquitin-like proteins as multifunctional signals. *Nat. Rev. Mol. Cell Biol.*, **6**, 599–609.

24. Kulka,R.G., Raboy,B., Schuster,R., Parag,H.A., Diamond,G., Ciechanover,A. and Marcus,M. (1988) A Chinese hamster cell cycle mutant arrested at G2 phase has a temperature-sensitive ubiquitin-activating enzyme, E1. *J. Biol. Chem.*, **263**, 15726–15731.
25. Quadrini,K.J. and Bieker,J.J. (2006) EKLF/KLF1 is ubiquitinated *in vivo* and its stability is regulated by activation domain sequences through the 26S proteasome. *FEBS Lett.*, **580**, 2285–2293.
26. Hu,C.D., Chinenov,Y. and Kerppola,T.K. (2002) Visualization of interactions among bZIP and Rel family proteins in living cells using bimolecular fluorescence complementation. *Mol. Cell*, **9**, 789–798.
27. Nagai,T., Ibata,K., Park,E.S., Kubota,M., Mikoshiba,K. and Miyawaki,A. (2002) A variant of yellow fluorescent protein with fast and efficient maturation for cell-biological applications. *Nat. Biotechnol.*, **20**, 87–90.
28. Carrere,S., Verger,A., Flourens,A., Stehelin,D. and Duterquecoquillaud,M. (1998) Erg proteins, transcription factors of the ets family, form homo, heterodimers and ternary complexes via 2 distinct domains. *Oncogene*, **16**, 3261–3268.
29. Mo,Y., Vaessen,B., Johnston,K. and Marmorstein,R. (2000) Structure of the Elk-1-DNA complex reveals how DNA-distal residues affect ETS domain recognition of DNA. *Nat. Struct. Biol.*, **7**, 292–297.
30. Murata,S., Chiba,T. and Tanaka,K. (2003) CHIP: a quality-control E3 ligase collaborating with molecular chaperones. *Int. J. Biochem. Cell. Biol.*, **35**, 572–578.
31. Murata,S., Minami,Y., Minami,M., Chiba,T. and Tanaka,K. (2001) CHIP is a chaperone-dependent E3 ligase that ubiquitylates unfolded protein. *EMBO Rep.*, **2**, 1133–1138.
32. Demand,J., Alberti,S., Patterson,C. and Höhfeld,J. (2001) Cooperation of a ubiquitin domain protein and an E3 ubiquitin ligase during chaperone/proteasome coupling. *Curr. Biol.*, **11**, 1569–1577.
33. Zhou,S. and Dewille,J.W. (2007) Proteasome-mediated CCAAT/enhancer-binding protein delta (C/EBPdelta) degradation is ubiquitin-independent. *Biochem. J.*, **405**, 341–349.
34. Asher,G. and Shaul,Y. (2005) p53 proteasomal degradation: poly-ubiquitination is not the whole story. *Cell Cycle*, **4**, 1015–1018.
35. Dice,J.F. (2007) Chaperone-mediated autophagy. *Autophagy*, **3**, 295–299.
36. Kim,C.A., Phillips,M.L., Kim,W., Gingery,M., Tran,H.H., Robinson,M.A., Faham,S. and Bowie,J.U. (2001) Polymerization of the SAM domain of TEL in leukemogenesis and transcriptional repression. *EMBO J.*, **20**, 4173–4182.
37. Seidel,J.J. and Graves,B.J. (2002) An ERK2 docking site in the Pointed domain distinguishes a subset of ETS transcription factors. *Genes Dev.*, **16**, 127–137.
38. Bachelor,A.H., Piper,D.E., de la Brousse,F.C., McKnight,S.L. and Wolberger,C. (1998) The structure of GABPalpha/beta: an ETS domain- ankyrin repeat heterodimer bound to DNA. *Science*, **279**, 1037–1041.
39. Lee,G.M., Donaldson,L.W., Pufall,M.A., Kang,H.S., Pot,I., Graves,B.J. and McIntosh,L.P. (2005) The structural and dynamic basis of Ets-1 DNA binding autoinhibition. *J. Biol. Chem.*, **280**, 7088–7099.
40. Mo,Y., Vaessen,B., Johnston,K. and Marmorstein,R. (1998) Structures of SAP-1 bound to DNA targets from the *E74* and c-*fos* promoters: insights into DNA sequence discrimination by Ets proteins. *Mol. Cell*, **2**, 201–212.
41. Maira,S.M., Wurtz,J.M. and Wasylyk,B. (1996) Net (erp/sap2), one of the ras-inducible tcfs, has a novel inhibitory domain with resemblance to the helix-loop-helix motif. *EMBO J.*, **15**, 5849–5865.
42. Stinson,J., Inoue,T., Yates,P.R., Clancy,A., Norton,J.D. and Sharrocks,A.D. (2003) Regulation of TCF ETS-domain transcription factors by helix-loop-helix motifs. *Nucleic Acids Res.*, **31**, 4717–4728.
43. Yates,P.R., Atherton,G.T., Deed,R.W., Norton,J.D. and Sharrocks,A.D. (1999) Id helix-loop-helix proteins inhibit nucleoprotein complex formation by the TCF ETS-domain transcription factors. *EMBO J.*, **18**, 968–976.
44. Teo,H., Perisic,O., González,B. and Williams,R.L. (2004) ESCRT-II, an endosome-associated complex required for protein sorting: crystal structure and interactions with ESCRT-III and membranes. *Dev. Cell*, **7**, 559–569.
45. Hu,W., Philips,A.S., Kwok,J.C., Eisbacher,M. and Chong,H.C. (2005) Identification of nuclear import and export signals within Fli-1: roles of the nuclear import signals in Fli-1-dependent activation of megakaryocyte-specific promoters. *Mol. Cell. Biol.*, **25**, 3087–3108.
46. Misteli,T. (2008) Physiological importance of RNA and protein mobility in the cell nucleus. *Histochem. Cell Biol.*, **129**, 5–11.
47. Boros,J., Donaldson,I.J., O'Donnell,A., Odrowaz,Z.A., Zeef,L., Lupien,M., Meyer,C.A., Liu,X.S., Brown,M. and Sharrocks,A.D. (2009) Elucidation of the ELK1 target gene network reveals a role in the coordinate regulation of core components of the gene regulation machinery. *Genome Res.*, **19**, 1963–1973.